JACS
JOURNAL OF THE AMERICAN CHEMICAL SOCIETY

Article

pubs.acs.org/JACS

Role of Environment for Catalysis of the DNA Repair Enzyme MutY

Elizabeth Brunk,[†] J. Samuel Arey,[‡,§] and Ursula Rothlisberger*[,†]

[†]Laboratory of Computational Chemistry and Biochemistry, Ecole Polytechnique Fédérale de Lausanne (EPFL), CH-1015 Lausanne, Switzerland

[‡] Environmental Chemistry Modeling Laboratory, Ecole Polytechnique Fédérale de Lausanne (EPFL), CH-1015 Lausanne, Switzerland

[§] Department of Environmental Chemistry, Swiss Federal Institute of Aquatic Science and Technology (Eawag), CH-8600 Dubendorf, Switzerland

Supporting Information

ABSTRACT: Control of the N-glycosylase reaction by the DNA repair enzyme, MutY, entails the organization of solvent molecules. Classical molecular dynamics and QM/MM simulations were used to investigate the solvent and environment effects contributing to catalysis. Our findings suggest that the entire reaction is an energetically neutral process, in which the first step is rate determining, requiring protonation of adenine (N_7) to initiate cleavage, and the second step is strongly exothermic, involving hydrolysis of an oxacarbenium ion intermediate. Although water molecules are catalytically active in both steps, the first step requires an entirely different level of solvent organization compared to the second. Needed to secure protonation at N_7, a long-term solvation pattern is established which facilitates the involvement of three out of the five structured water molecules in the active site. This persistent arrangement coordinates the catalytically active water molecules into prime positions to assist the proton transfer: (i) a water molecule frequently bridges the catalytic residues and (ii) the bridging water molecule is assisted by 1−2 other 'supporting' water molecules. To maintain this configuration, MutY, surprisingly, uses hydrophobic residues in combination with hydrophilic residues to tune the microenvironment into a 'water trap'. Hydrophilic residues prolong solvent residence times by maintaining hydrogen-bonding networks, whereas the hydrophobic residues constrain the positioning of the catalytic water molecules that assist the proton-transfer event. In this way, the enzyme uses both entropic and enthalpic considerations to guide the water-assisted reaction.

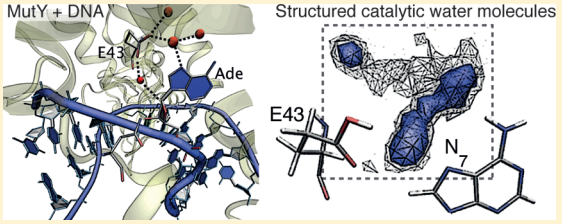

INTRODUCTION

Cells have developed elaborate repair systems to defend themselves against unwarranted and detrimental mutations in DNA. One of the central machineries that is able to uphold the integrity of cellular DNA, despite constant threats of stress from the environment, is that of base excision repair (BER) proteins. The most common form of oxidative damage repaired by BER proteins is the 8-oxo-guanine (OG) lesion, resulting from the attack of highly reactive hydroxyl radicals on the C_8 atom. Consequently, OG preferentially binds to adenine (OG:A),[1,2] leading to a high rate of G-C to T-A transversion mutations during DNA replication.[3] The OG lesion and its resulting mispairs are effectively handled by a suite of interacting proteins, named the 'GO' system, which involve the MutM, MutT, and MutY enzymes.[2,4] Among these, MutY plays a key role in the recognition of OG:A, the excision of the mispaired adenine base, and the protection of the 'empty' apurinic site after excision has taken place.[5]

Crystallographic structures and transition-state (TS) analysis using kinetic isotope effects (KIEs) have provided key insights into the mechanism adopted by MutY to excise the mispaired adenine base. The *Bacillus stearothermophilus* MutY (bMutY) crystal structure[6] demonstrates that residues intercalate the double helix, resulting in the expulsion of adenine into an extrahelical cavity of the protein. Once inside the cavity, the glycosidic bond of adenine is cleaved as a result of key interactions with the residues lining the pocket, illustrated in Figure 1a. Cleavage of the adenine and ribose moieties results in the formation of an oxacarbenium ion intermediate, which can then be hydrolyzed to generate the empty apurinic site.[6] From these structural insights, a S_N1 mechanism, described in Figure 1b, has been proposed in which a nearby glutamate residue (E43 in bMutY) initiates cleavage by transferring its proton to the adenine base at N_7.

Further support of a S_N1 reaction comes from KIEs, indicating that *Escherichia coli* MutY (eMutY) adopts a $D_NA_N^{\ddagger}$ mechanism for the excision of adenine.[7] Such a mechanism involves a scheme in which the glycosidic bond breaks and forms repeatedly before the irreversible nucleophilic addition reaction takes place. Consistent with the evidence that suggests N_7 to be protonated, KIEs suggest that protonation occurs in a pre-equilibrium step before cleavage.[7,8] By preceding the cleavage of the glycosidic bond, protonating N_7 may be a

Received: February 21, 2012
Published: April 26, 2012

   dx.doi.org/10.1021/ja301714j | J. Am. Chem. Soc. 2012, 134, 8608−8616

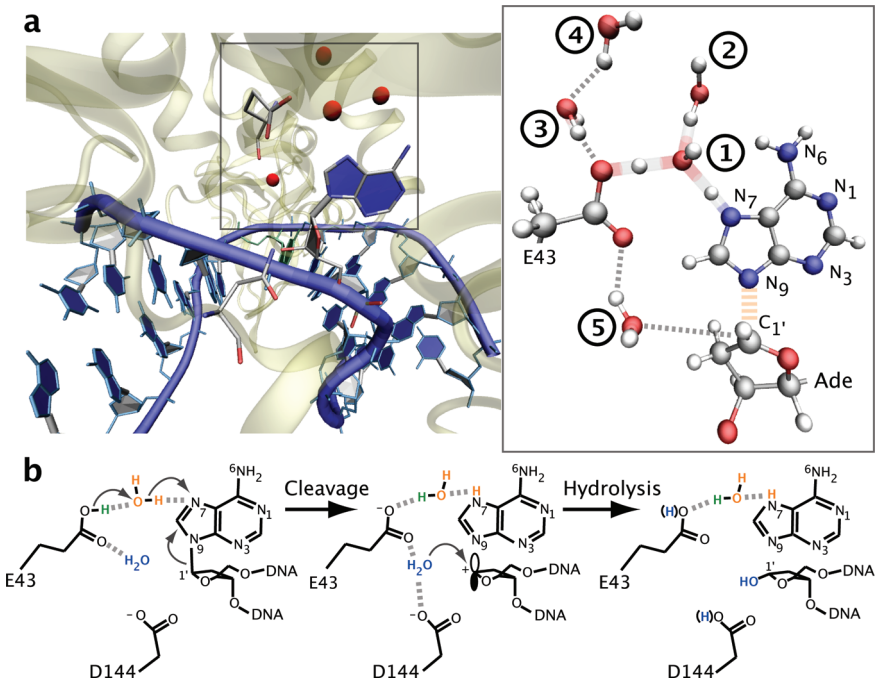

Figure 1. (a) The mispaired adenine is extruded into an extrahelical cavity, shown on the left. The catalytic site (magnified panel on the right) displays five water molecules (wat1, wat2, wat3, wat4, and wat5), present during the cleavage reaction. As shown in cartoon representation, a concerted proton transfer occurs from E43 to N_7, mediated by a water molecule in the vicinity of the catalytic pocket, during cleavage. The proton is transferred through a bridging water molecule, wat1, supported by neighboring structured water molecules from above, wat2 and wat3. (b) The previously proposed reaction mechanism of MutY, inferred from key insights from crystallographic structures and kinetic isotope studies. The putative mechanism is a S_N1 reaction in which the cleavage of the glycosidic bond takes place after a proton (green) is transferred from E43 through a nearby water molecule (orange) to N_7 of adenine. The hydrolysis step, catalyzed by a second water molecule (in blue), takes place after the formation of the oxacarbenium ion intermediate. Both steps involve the direct participation of a catalytic water molecule.

critical event to enable departure of adenine, as suggested by experiments with substrate analogues[9] and KIE measurements.[7,10]

Interactions involving other nitrogen atoms of adenine may also be important during the cleavage reaction. Evidence from KIEs suggests that N_6 undergoes a loss of hydrogen bonding and/or solvation at the TS.[7] Enzyme interactions with N_1 and N_3 may also facilitate the departure of the adenine leaving group.[10,11] During acid-catalyzed dAMP hydrolysis, adenine is reported to be diprotonated (N_1 and N_7) at the TS.[12] The catalytic effect of double protonation on glycosidic bond cleavage was revealed in N-riboside hydrolysis,[13] and the conditions for which adenine and other base pairs are protonated and diprotonated have been studied extensively.[14−18] However, whether adenine protonation or diprotonation occurs in MutY and its impact on cleavage remains unclear.

Direct involvement of solvent interactions with adenine can be deduced from crystal structures.[6,19,20] Both bMutY and eMutY crystal structures reveal five to six structured water molecules in the vicinity of E43 and N_7, illustrated in Figure 2. One proposed role for water molecules in this region is to form a 'water bridge,' connecting the E43 and adenine moieties.[6] Since adenine is too far from E43 (4−5 Å) to accept a proton via direct transfer, at least one water molecule is needed to 'relay' the proton in the initial protonation event at N_7.[6,7,10] Another proposed role for a nearby water molecule is to hydrolyze the oxacarbenium ion intermediate. Therefore, at least one water molecule is directly involved in both cleavage and hydrolysis steps.

Missing from this description are the inner workings of the enzyme reaction mechanism and, in particular, the respective roles of different water molecules for catalysis. Comparing the three crystal structures in Figure 2 suggests that the ordering of water molecules in the vicinity of E43 and N_7 may be an important factor, since similar numbers and arrangements of water molecules are conserved despite different crystallization conditions and procedures. However, whether all five structured water molecules are truly conserved and involved in catalysis is a question that requires analysis extending beyond a comparison of crystal structures. The present contribution aims to establish the characteristic functions of the catalytically active water molecules in addition to other environmental factors which may influence catalysis and to probe Nature's strategy for securing the involvement of solvent molecules in water-assisted chemical reactions.

METHODS

Classical molecular dynamics simulations were performed starting from the bMutY crystal structure.[6] The mutation D144N induced during crystallization was manually reverted back to the native sequence. Parameters for the OG moiety and the $[FeS]_4$ cluster were based on the parametrization of Miller et al.[21] Using PROPKA,[22−24] we estimated that all of the residues adopt the default protonation states with the possible exception of E43 (pK_a of 6.7), which is surrounded by a 5 Å sphere of hydrophobic residues (I191, V39, L134, V44, Y126, L46, V144, and W30 for bMutY). Simulations were performed for both protonated and unprotonated states of E43 and D144. Each structure was solvated with TIP3P water and, depending on the total charge of the system, either 28, 29, or 30 K^+ ions, achieved system neutrality, in an orthothrombic periodic box (90 × 98 × 120 Å). The particle mesh Ewald (PME) method, with a nonbonded cutoff

dx.doi.org/10.1021/ja301714j | J. Am. Chem. Soc. 2012, 134, 8608−8616

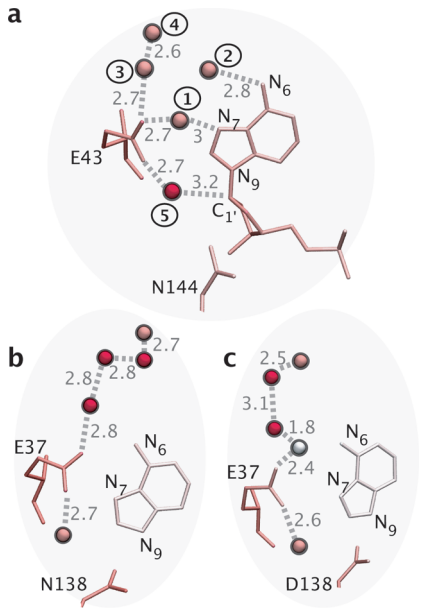

Figure 2. (a) The *Bacillus stearothermophilus* MutY crystal structure (pdb entry 1RRQ), with 5 structured waters in the 5 Å vicinity of N_7 and E43. The residues are colored by B-factor, indicating which belong to a part of the structure that is well-ordered. The lowest B-factors correspond to higher order, shown in red, whereas the higher B-factors correspond to less order, shown in gray. (b,c) Water molecules in the 5 Å vicinity of E37 show a similar patter in *Escherichia coli* MutY (pdb entries 1MUD and 1WEI, respectively). In both of these cases, the adenine substrate is in complex with MutY crystal structure, which may explain the slight variation in order and lack of a bridging water molecule. Additionally, variations in the point mutation D144/D138 in bMutY and eMutY, respectively, might also affect the structure of water molecules in the vicinity of the $C_{1'}$ on the glycosyl ring. Yet, despite these differences in crystallization protocols and procedures, the B-factors for these water molecules are still lower compared to those of most of the semistructured solvent molecules.

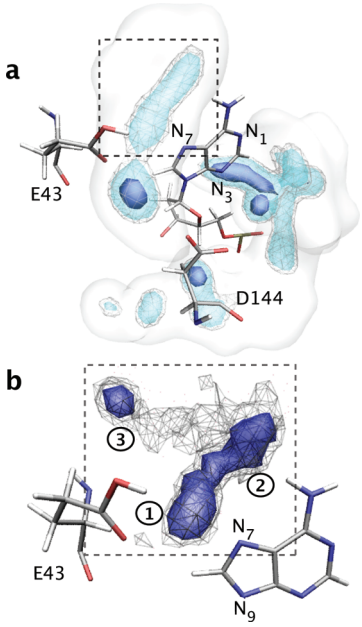

Figure 3. (a) The solvent distribution within 10 Å of adenine in the active site is represented by a contour plot, depicting the probability to find water molecules at a given position during the classical molecular dynamics simulations. The positions of the water molecules were binned using a distance of 0.5 Å between grid points. The number of water molecules that passed through each grid element was computed, and this density was represented using a Gaussian broadened distribution with width equal to 1 Å. The lighter and darker blue regions correspond to frequently occupied locations of solvent molecules throughout the trajectory (contour levels of 0.5 and 0.8, respectively). One of the locations most frequently occupied is consistent with the position of the nucleophilic water molecule, positioned 3−4 Å from the $C_{1'}$ in the crystal structures. (b) The maximally occupied positions of water molecules in the 5 Å vicinity of N_7 and E43 when a water molecule is bridging the catalytic residues (70% of the time). These three maxima, illustrated in dark blue (contour level of 0.5), correspond to positions of three out of five structured water molecules in the bMutY crystal structure. This configuration is the most persistent arrangement of water molecules in the vicinity of N_7 and E43 throughout the entire classical molecular dynamics simulation.

of 12 Å, was used with periodic boundary conditions and the Langevin piston Nosé−Hoover method[25−27] to ensure constant pressure and temperature conditions. For each system, NAMD molecular dynamics[28] was performed, using the AMBER[29] 99sb force field[30,31] for 17−25 ns. For the QM/MM simulations, we use an extension of Car−Parrinello molecular dynamics (CPMD)[32,33] and describe the QM atoms by norm-conserving Martins−Trouiller pseudopotentials[41] with dispersion-corrected atom-centered potentials[42−45] and the DFT/BLYP functional,[34,35] which has been applied to many hydrogen-bonded systems.[36−40] The QM atoms include the adenine base, the ribose and phosphate moieties, capped at the O−$C_{5'}$ bond of the neighboring base with a monovalent pseudopotential,[46] E43 and D144, capped at the amide backbone of the neighboring residues, and four catalytic water molecules. The wave functions are expanded in a plane wave basis set with a 70 Ry cutoff inside a orthorhombic quantum box with dimensions 39 × 42 × 34 $Å^3$. Long-range interactions were decoupled using the Martyna−Tuckerman scheme.[47] The MM subset is described by a classical AMBER 99sb force field and contains the rest of the protein and DNA and explicit solvent water molecules and 30 counterions. The QM/MM simulations were performed at constant pressure and temperature, using a Nosé−Hoover thermostat. The system was equilibrated for 10 ps before performing constrained molecular dynamics simulations for thermodynamic integration.[48,49] Constraints were employed to fix the reaction coordinate at various distances (in increments of 0.1 Å). Each constrained distance was sampled for 2.5 and 3.5 ps near and at the barrier, respectively.

Table 1. Radial Pair Distributions for N_1, N_3, N_7, and N_9 of Adenine and Solvent Molecules[a]

atom	solvation shell (Å)	number of water molecules	average residence time (% of total trajectory)
N_7	2.5	1.0	45
N_7	3.7	4.6	100
N_3	2.3	0.8	13
N_3	5.9	17.1	40
N_9	3.6	1.5	1.1
N_9	4.3	3.7	4.4
N_1	2.6	0.1	0.1
N_1	4.9	9.0	36

[a]The number of water molecules in the first and second solvation shell is given for each atom. The average residence time of water molecules within these shells has been computed and is given by the percent of time the water molecule occupies the first and second solvation shells.

RESULTS AND DISCUSSION

Structured Water Molecules in the Active Site. Do the structured water molecules in the active site persist in solution?

dx.doi.org/10.1021/ja301714j | J. Am. Chem. Soc. 2012, 134, 8608−8616

Table 2. Solvent Occupancies for Catalytic Water Molecules in the Vicinity of E43 and N_7 [a]

	percent of total 25 ns trajectory (%)
water molecule bridging E43/N_7	72
water molecule ≤2 Å from bridge	53
water molecule ≤3 Å from bridge	93
protonated E43 donates H-bond	70

[a]Computed are the percentages of the trajectory in which specific characteristic ordering of water molecules are found. A water molecule is considered to be in a bridging position when it is within hydrogen-bonding distances to both E43 and N_7 (within 1.8 Å). Water molecules considered to 'support' the bridging water molecule were within 2−3 Å of the bridging water molecule. Evaluated at each bridging event is whether E43 acts as a hydrogen-bond donor or acceptor.

If so, in what characteristic positions and orientations? Starting from the bMutY crystal structure, we performed classical molecular dynamics simulations to study the DNA-bound MutY protein in an explicit solvent environment. Evaluating the distribution of water molecules during 25 ns, we find that specific regions surrounding adenine have increased occupancies compared to others, illustrated by the contour plot in Figure 3a. The region surrounding N_1 and N_3 accommodates the highest number of water molecules, yet minimal hydrogen bonding occurs (during 1% of the trajectory with average lifetimes of 7.5 ps) with adenine at these positions. Another highly occupied region is in the vicinity of the $C_{1'}$ atom of the glycosyl ring, which is the location of a structured water molecule, proposed to act as nucleophile during hydrolysis (see wat5 in Figure 2a and in Figure S1, Supporting Information). In contrast, a lower density of water molecules populates the vicinity of E43 and N_7, yet a significant amount hydrogen bonding occurs, with notably longer lifetimes, with adenine at this location (Table 1 and Figure S2, Supporting Information). These findings are consistent with base-opening studies, which similarly show long-lived water binding sites in the vicinity of the N_7 atom of the open adenine base.[50]

While the 5 Å vicinity of E43 and N_7 accommodates five solvent molecules throughout the simulation (Figure 2a), only three water molecules remain in the catalytic site during the entire simulation. The long residence times for these solvent molecules are found in the most persistent configuration, in which water molecules occupy predominantly three distinct

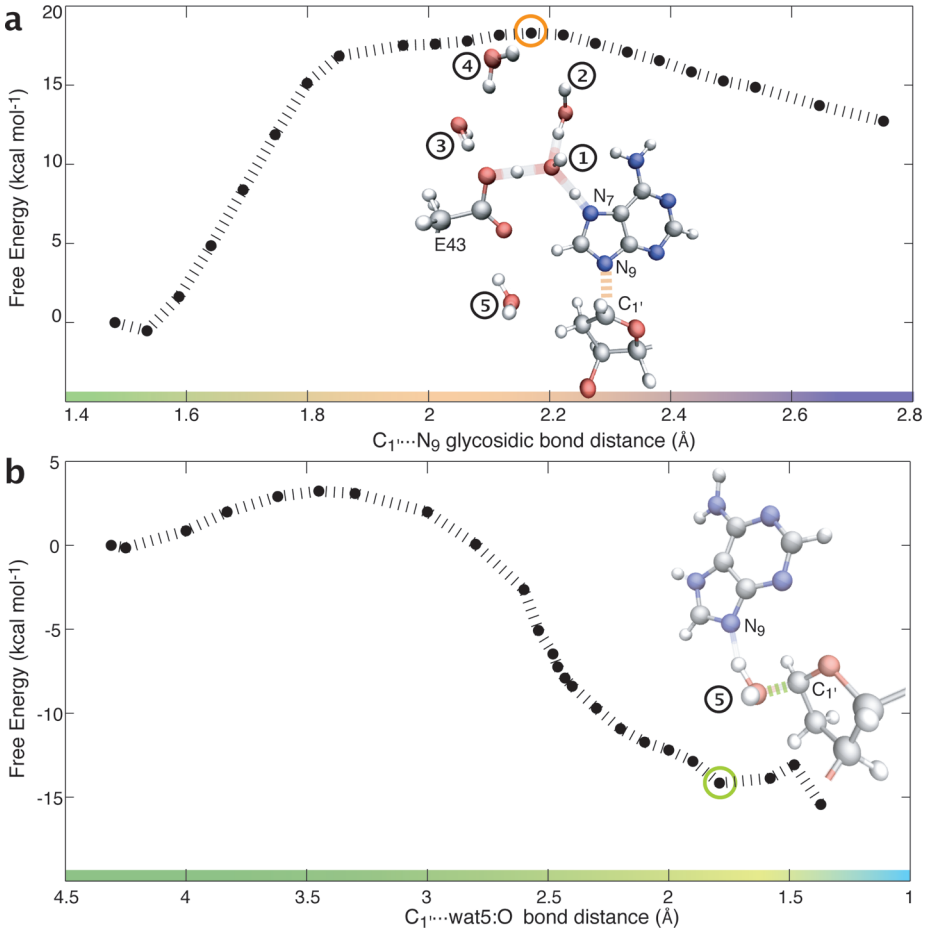

Figure 4. Free energy profiles for the first and second catalytic steps in (a) and (b), respectively. The first step is represented by the elongation of the N_9···$C_{1'}$ bond length. The bond length is constrained at various distances, and the averaged force on the constraint is integrated over the change in reaction coordinate to obtain the free energy. At a glycosidic bond length of 1.9 Å, a spontaneous, concerted proton transfer occurs from E43 to N_7, mediated by a bridging water molecule. The proton exchanges reversibly between N_7, wat1, and E43 within a range of glycosidic bond distances (1.9 to 2.3 Å), indicated by the orange circle. (b) A water molecule (wat5) in the 4 Å vicinity of the glycosyl moiety hydrolyzes the positive $C_{1'}$ carbon center. At a $C_{1'}$···wat5:O bonding distance of 1.4 Å, a concerted proton transfer occurs from the water molecule to N_9 of adenine, represented by the slight 1−2 kcal mol^{-1} barrier. The proton exchanges reversibly, indicated by the light-green circle, before becoming fully attached to N_9.

dx.doi.org/10.1021/ja301714j | J. Am. Chem. Soc. 2012, 134, 8608−8616

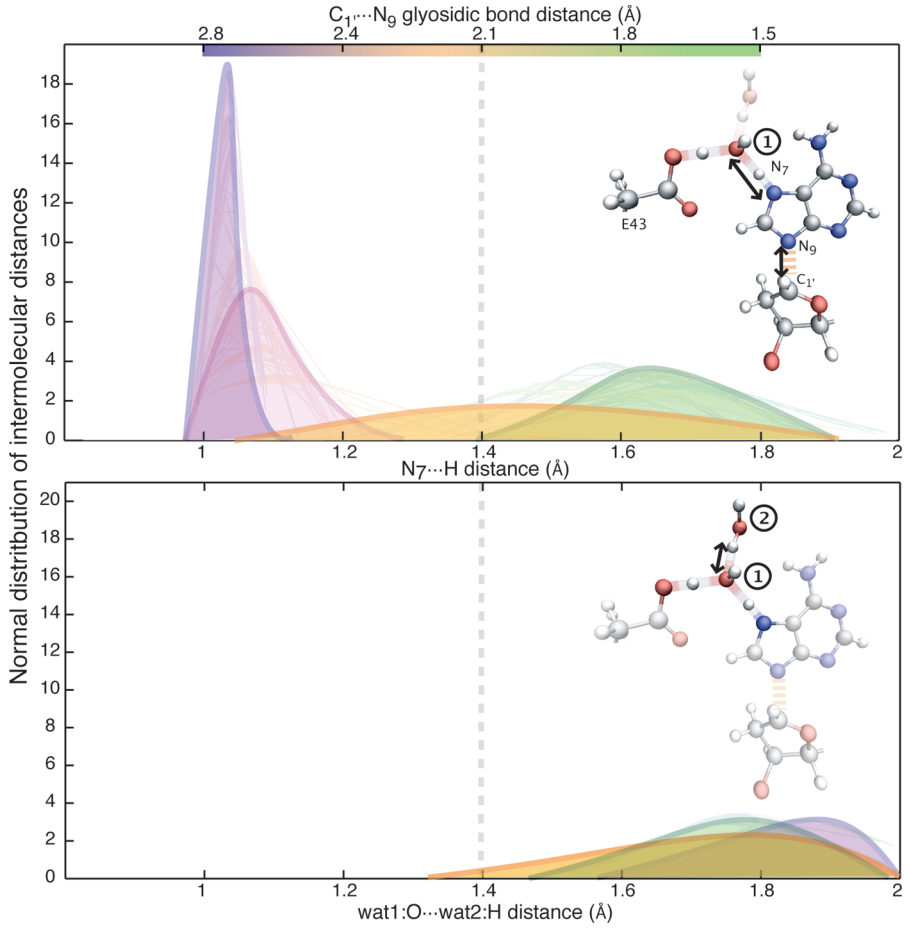

Figure 5. Using a histogram analysis, the magnitude of the fluctuation in the distance varies at different points along the reaction coordinate. To better visualize these fluctuations, a normal (Gaussian) distribution was used to describe the changes in intermolecular distances between N_7···wat1:H (top) and wat1:O···wat2:H (bottom) along the reaction coordinate (see Figure S11, Supporting Information). The height of the Gaussians represents the probability of finding the atoms at a given separation distance, whereas the spread of the Gaussians represents the magnitude in fluctuation of the bonding distance at a given point in the reaction coordinate. The bond distributions are averaged over the thermodynamically equilibrated windows and colored according to N_9–$C_{1'}$ bond distance (green, orange, and violet represent N_9–$C_{1'}$ distances ranging from 1.48 to 2.0, 2.1 to 2.3, and 2.4 to 3 Å, respectively). Elongation of the glycosidic bond induces changes in bonding distributions around the TS. The largest spread in distribution of N_7···wat1:H bonding distances occurs just before the TS (a N_9–$C_{1'}$ distance of 1.9–2.2 Å), in which the atoms adopt distances as small as 1.07 and as large as 1.9 Å from one another (orange curve). Similarly, the broadest distribution in bonding distance between wat1:H···wat2:O occurs at this same point in the trajectory, when the proton is 'in transit' from E43 to N_7. Assisting wat1 during the proton transfer, wat2 interacts strongly via hydrogen bonds, adopting distances as small as 1.3 Å.

positions (Figure 3 (b)). This configuration is consistent with data that suggest a proton is transferred to N_7 via a nearby water molecule,[6] as position 'one' coordinates a water molecule into the prime location to bridge E43 and N_7. Indeed, a bridging water molecule is consistently found at position 'one' 72% of the time, and one to two other water molecules are found either within hydrogen-bonding distance or within 3 Å of the bridging water molecule in 53% and 93% of the cases, respectively (see wat1, wat2, and wat3 in Figure 2a and Table 2). While occasional exchanges with bulk solvent occur in the active site, the same three water molecules consistently populate this configuration, and one out of the three is found in the bridging position 67% of the time. Thus, three out of the five structured water molecules have long residence times, which can be attributed to the most persistent, or optimal, arrangement of solvent molecules in the reactant state.

What factors are responsible in securing a bridging water molecule? The probability of finding a water molecule in this position is influenced by a protonated E43, which donates a hydrogen bond to the bridging water molecule 70% of the time. We studied the sensitivity of the system to changes in pH by varying the protonation states of E43 and D144, which results in overall different solvent distributions (Figure S3, Supporting Information). Despite these differences, persistence of the same subset of water molecules in the active site remains consistent. Yet, while residence time appears to be independent of changes in protonation state, the probability to find a bridging water molecule is highest for a system with E43 protonated and D144 unprotonated (Table S1 and Figure S4, Supporting Information).

How are residence times upheld to maintain a unique configuration? The nature of the microenvironment surrounding the catalytic site may contribute to the long residence times of the water molecules. Alternating shells of hydrophobic and hydrophilic residues surround the active site in various crystal structures (see Figures S5 and S6, Supporting Information). This pattern suggests that the structure–function relationship of residues in this region of the MutY protein, and perhaps in other glycosylases where solvent plays an integral role in catalysis, has evolved into a 'water trap,' increasing the

dx.doi.org/10.1021/ja301714j | J. Am. Chem. Soc. 2012, 134, 8608–8616

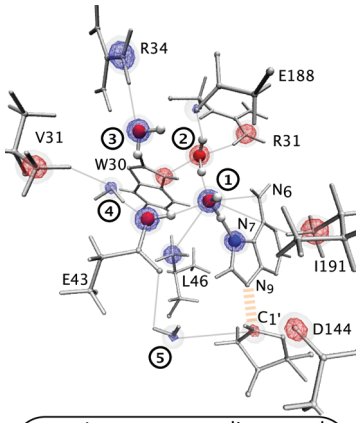

strong		medium–weak	
I191···wat1	0.82	V31···wat4	0.43
E43···wat1	−0.80	D144···wat5	0.36
E43(O)···H	−0.79	E43···wat4	−0.24
W30···wat2	0.75	$C_{1'}$···wat5	0.21
L46···wat1	−0.72	E43···wat5	−0.18
E43···wat3	−0.71	E188···wat2	−0.16
N_7···wat1	−0.71	N_6···wat1	−0.09
R34···wat3	−0.71		
wat1···wat2	0.65		
R31···wat2	0.65		

Figure 6. A Pearson-like correlation coefficient was used to measure of the strength of the coupling between the change in reaction coordinate (N_9···$C_{1'}$ bond length) and the interaction distances of the five different water molecules with various residues lining the active site. A contour plot was generated to visualize the strongest correlating residues by placing spherical Gaussians, representing the correlation coefficient, on the respective interacting atom center. Stronger correlation is represented by larger spheres in the contour plot, depicting the interactions which are the most cooperative to the increase in reaction coordinate. The most cooperative interactions involve wat1, wat2, and wat3. Surprisingly, some residue−solvent interactions that also correlate strongly to reaction coordinate correspond to hydrophobic residues, positioned at the site of N_7 protonation to interact with wat1 during proton transfer.

likelihood that water molecules contribute to the water-assisted chemical reaction.

Water-Mediated Cleavage Reactions. Do these structured water molecules contribute to catalysis? Starting from the classically equilibrated structure, we studied the catalytic cycle of MutY using QM/MM CPMD simulations.[32,33,51] Testing the putative stepwise S_N1 mechanism described in Figure 1b, the overall reaction was examined in two steps: (i) cleavage of the glycosidic bond and (ii) hydrolysis of the oxacarbenium intermediate. We have chosen to describe cleavage with a single reaction coordinate, the N_9···$C_{1'}$ bond length. Starting from the equilibrium value of 1.48 ± 0.2 Å, the reaction coordinate was systematically increased to 2.8 Å. This approach utilizes a minimal reaction coordinate to study the stepwise reaction of MutY while allowing all other degrees of freedom to relax. Using thermodynamic integration (TI),[48,49] the barrier for cleavage is found to be 18 ± 1.6 kcal mol^{-1} (Figure 4a and Figure S10, Supporting Information).

Cleavage of the glycosidic bond induces several significant molecular events, assisted by water molecules. Lengthening the N_9···$C_{1'}$ bond induces a spontaneous proton transfer from E43 to N_7, mediated by the water molecule (wat1) that bridges these residues. Our findings are consistent with previous data which suggest that a proton transfer to N_7 pre-empts the glycosidic-bond cleavage.[6,7] During this pre-equilibrium period (N_9···$C_{1'}$ bond length of 1.9−2.3 Å), proton exchanges among E43, wat1, and N_7 are concerted and reversible. While the proton is 'in transit' between E43 and N_7, wat1 is supported by hydrogen-bond donors, N_6 of adenine and a nearby water molecule (wat2). At the TS, these interactions diminish, in agreement with $^{15}N_6$ KIEs.[7]

How do changes in the reaction coordinate influence the behavior of nearby water molecules? Examining the molecular events surrounding the proton transfer to N_7, three of the five structured water molecules in the 5 Å vicinity of N_7 are catalytically active, adopting either direct or indirect roles to assist catalysis. Molecular interactions among these water molecules and catalytic residues are identified by changes in bonding distributions, cooperative with the reaction coordinate (Figure 5). The largest spread in distribution occurs just before the proton transfers from E43 to wat1 (see the orange curve at the bottom of Figure 5), in which wat2 assists wat1, adopting hydrogen-bond distances as small as 1.3 Å (see the orange curve at the top of Figure 5). While wat1 directly assists cleavage, relaying a proton from E43 to N_7, wat2 and wat3 assist wat1 and E43, respectively. These events suggest that while certain structured water molecules are not directly involved in catalysis, they are more than mere bystanders and may enable MutY to overcome energetic barriers of a water-mediated proton transfer during cleavage.

Similar to these water molecules that are indirectly involved in catalysis, active site residues may also play secondary roles to assist the cleavage reaction. A Pearson-like correlation coefficient was used to measure the strength of relationships between reaction coordinate and intermolecular distances of residues and the respective water molecules in the 5 Å vicinity of N_7 (see eq S2, Supporting Information). The contour plot, shown in Figure 6, was generated to visualize the residues most affected by the change in reaction coordinate by representing the correlation coefficients with spherical Gaussians centered on their respective interacting atoms. The results reveal that interactions involving wat1, wat2, and wat3 are more cooperative with cleavage than those involving wat4 and wat5. As expected, hydrophilic residues (R31 and R34) strongly interact with wat2 and wat3 via hydrogen bonds, which may be one factor preserving their unique configuration. More surprising are the interactions that correlate most strongly, which involve two hydrophobic residues (I191 and L46 in bMutY) sitting opposite to one another at the site of N_7 protonation. Residues strategically placed at this site appear to aid the proton transfer by constraining the orientation of wat1. Furthermore, cooperative interactions involving W30 and wat2 may similarly manipulate the orientation of wat2 to assist wat1 during proton transfer. A similar motif is found in eMutY, in which hydrophobic residues, M185 and L40, guard the site of N_7 protonation (Figure S5, Supporting Information). Our findings suggest that the enzyme utilizes both hydrophilic and hydrophobic interactions to order and orient three catalytic water molecules during the proton transfer to N_7.

Nucleophilic Water attack. Does a similar pattern in solvent organization persist during hydrolysis? The QM/MM simulations indicate that the cleavage reaction generates a stable oxacarbenium ion intermediate (N_9···$C_{1'}$ bond length of 2.8 Å) and prepares and activates a water molecule (wat5) for the subsequent hydrolysis reaction. During cleavage, wat5 is held within 4−5 Å of the $C_{1'}$ atom by hydrogen-bonding interactions with E43 (Figure 1a) and becomes slightly

dx.doi.org/10.1021/ja301714j | J. Am. Chem. Soc. 2012, 134, 8608−8616

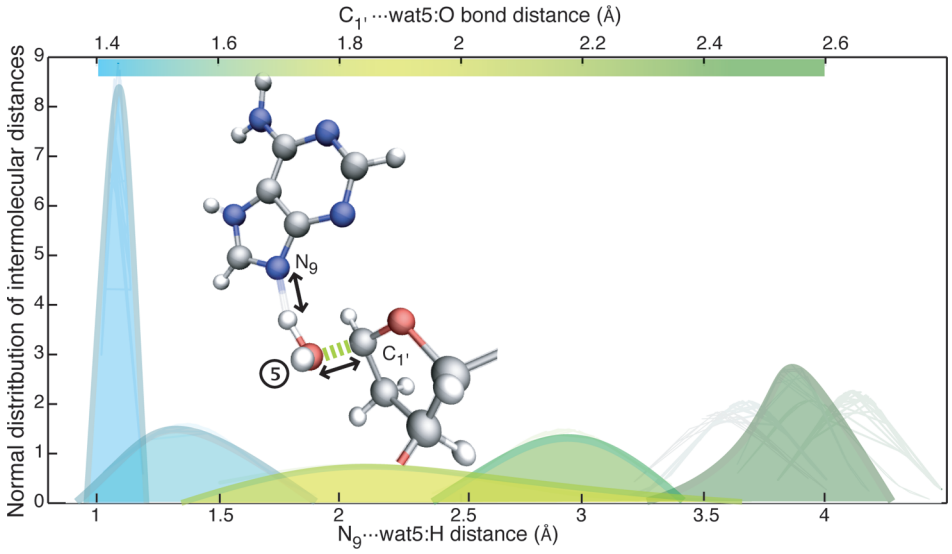

Figure 7. A normal (Gaussian) distribution was used to describe the changes in intermolecular interaction distances between monoprotonated adenine and the proton of wat5, N_9···wat5, cooperative with the decrease in $C_{1'}$···wat5 bond distance (see Figure S11, Supporting Information). The height of the Gaussians represents the probability of finding the atoms at a given separation distance, whereas the spread of the Gaussians represents the magnitude in fluctuation of the bonding distance at a given point in the reaction coordinate. The color shift from dark- to light-green to blue indicates the decrease in the $C_{1'}$···wat5 distance from 2.6 to 2.2, 2.1 to 1.7, and 1.6 to 1.3 Å, respectively. The normal distributions of N_9···wat5 reveal that the bonding distances are the most broad at a $C_{1'}$···wat5 bond distance of 1.8 Å, fluctuating by nearly 2 Å. At these $C_{1'}$···wat5 distances, the proton hops back and forth between the water molecule and N_9, as shown by the light-green curve.

polarized and properly oriented for an attack on the $C_{1'}$ as the oxacarbenium ion forms (Figure S7, Supporting Information). Formation of the oxacarbenium ion intermediate was confirmed by evaluating point charges, using a dynamic electrostatic potential (ESP) fitting procedure,[52] and the electron density, using a Voronoi analysis (see Supporting Information). Following a previous proposition,[6] we have chosen wat5, initially at a distance of 4.3 Å from the $C_{1'}$ atom, to catalyze the reaction. Diminishing the distance between the $C_{1'}$ atom and wat5 corresponds to a free energy profile that indicates that the hydrolysis reaction is strongly exothermic with a slight barrier of 3.2 ± 0.4 kcal mol^{-1} for breaking the hydrogen bond between the deprotonated E43 and wat5 (Figure 4b and Figure S10, Supporting Information). The hydrolyzed product is favored by 15.4 ± 1.5 kcal mol^{-1}, making the entire reaction (step 1 + step 2) almost energetically neutral. These findings indicate that cleavage is the rate-determining step and supports a $D_NA_N^{\ddagger}$ mechanism.[7]

Molecular interactions between wat5 and residues lining the route to the $C_{1'}$ atom, (E43, D144, and Y126), act as a 'water shuttle' to guide the water molecule to the site of hydrolysis. It has been suggested that E43 or D144 act as bases for the nucleophilic attack.[6,7,10] However, neither of these residues assumes this role during the simulation. Instead, monoprotonated adenine itself acts as the base to activate the nucleophilic water attack on $C_{1'}$. During the hydrolysis step, a spontaneous proton transfer occurs from wat5 to N_9 on adenine. Displayed in Figure 7, as the wat5 approaches the $C_{1'}$, the distribution of N_9···wat5 bond distances broadens to include distances as small as 1.4 and as large as 3.6 Å. The broadest distribution occurs when the proton hops back and forth between N_9 and wat5 (the light-green curve), represented by the slight 1−2 kcal mol^{-1} barrier in the free energy profile. Adenine is most likely to act as base, because wat5 is 4 Å away from E43 before it interacts with the positive $C_{1'}$ center, making a proton abstraction unlikely. While a hydrogen abstraction from wat5 is more likely to arise from D144, hydrogen-bonding interactions with Y126 prevent it from acting as more than simply a hydrogen-bond acceptor for wat5.

Configuration and residence times do not seem to play a role in hydrolysis, as they do during cleavage. In contrast, we do not observe strong correlations for water molecules, aside from wat5, or residues in the active site with the reaction coordinate during hydrolysis. Furthermore, classical molecular dynamics simulations indicate that the residence time of wat5 is not upheld in the reactant state, as water molecules at this position are frequently exchanged with bulk solvent. Despite these conditions, hydrolysis is still likely to occur as long as the vicinity of the glycosyl moiety is solvated, as indicated by the free energy profile (Figure 4b). Hence, conformation may be a factor only influencing catalytic efficacy in the first catalytic step, as water molecules must be effectively coordinated in a unique configuration to mediate the proton transfer to N_7 from E43.

■ CONCLUSIONS

Although water molecules are directly involved in both the cleavage and the hydrolysis steps, the first catalytic step, which is rate-determining and requires protonation of N_7, entails an entirely different level of solvent organization compared to the second. The involvement of water molecules during cleavage potentially enables MutY to lower the energetic barrier of a proton transfer, which contributes a catalytic rate enhancement equivalent to nearly half of the required activation energy.[7] In contrast, the hydrolysis step is strongly exothermic and requires minimal solvent organization, apart from orienting the nucleophilic water for its attack on the oxacarbenium ion intermediate. Our findings reveal that enzymatic efforts to convene solvent in an optimal configuration occur in the reactant state.

To secure protonation at N_7, a long-term solvation pattern is established, which facilitates the involvement of three out of the

dx.doi.org/10.1021/ja301714j | J. Am. Chem. Soc. 2012, 134, 8608−8616

five structured water molecules in the vicinity of E43 and N_7. This persistent arrangement coordinates the catalytically significant water molecules into three prime positions for a proton transfer: (i) a position bridging the catalytic residues, E43 and N_7; (ii) a position that assists the bridging water molecule; and (iii) one that assists E43 during the proton-transfer event. Thus, preserving an ideal arrangement of three water molecules may direct the course of catalysis for the cleavage reaction and enables the control of the water-assisted reaction.

How does an enzyme secure a unique configuration of solvent molecules? As expected, hydrophilic residues form strong hydrogen-bonding interactions with the structured water molecules, which may be one factor preserving their unique configuration and prolonging their residence times. More surprising are the interactions with hydrophobic residues, which constrain the positioning of the catalytic water molecules that assist the proton-transfer event during cleavage. In this way, enzymatic control uses both entropic and enthalpic considerations to guide the reaction.

■ ASSOCIATED CONTENT

Supporting Information

Further details of the QM/MM and classical simulations, Figure S1−S11, Table S1, comparisons of the arrangement of water molecules in various crystal structures of MutY, comparisons of active sites with alternating hydrophobic and hydrophilic patterns for bMutY and eMutY, details of the contour plots, and the Voronoi analysis and d-RESP charges for the oxacarbenium ion intermediate. This material is available free of charge via the Internet at http://pubs.acs.org.

■ AUTHOR INFORMATION

Corresponding Author

ursula.roethlisberger@epfl.ch

Notes

The authors declare no competing financial interest.

■ ACKNOWLEDGMENTS

The authors gratefully acknowledge funding (to J.S.A.) from the U.S. National Science Foundation MPS-DRF award 0502600 and from the Swiss National Science Foundation award 200020-130082 as well as the DIT (EPFL) and the Swiss National Computing Center (CSCS) for the generous computing grants. We also thank Prof. Michele Cascella and Dr. I-Chun Lin for early input in the project.

■ REFERENCES

(1) Tchou, J.; Kasai, H.; Shibutani, S.; Chung, M. H.; Laval, J.; Grollman, A. P.; Nishimura, S. *Proc. Natl. Acad. Sci. U.S.A.* **1991**, *88*, 4690−4694.
(2) Tchou, J.; Grollman, A. P. *Murat. Res.* **1993**, *229*, 277−287.
(3) Cabrera, M.; Ngheim, Y.; Miller, J. H. *J. Bacteriol.* **1988**, *170*, 5405−5407.
(4) Michaels, M. L.; Miller, J. H. *J. Bacteriol.* **1992**, *174*, 6321−6325.
(5) Michaels, M. L.; Tchou, J.; Grollman, A. P.; Miller, J. H. *Biochemistry* **1992**, *31*, 10964−10968.
(6) Fromme, J. C.; Banerjee, A.; Huang, S.; Verdine, G. *Nature* **2004**, *427*, 1476−1122.
(7) McCann, J. A. B.; Berti, P. J. *J. Am. Chem. Soc.* **2008**, *130*, 5789−5797.
(8) Kampf, G.; Kapinos, L. E.; Griesser, R.; Lippert, B.; Sigel, H. *J. Chem. Soc., Perkin Trans.* **2002**, *2*, 1320−1327.
(9) Bulychev, N. V.; Varaprasad, C. V.; Dorman, G.; Miller, J. H.; Eisenberg, M.; Grollman, A. P.; Johnson, F. *Biochemistry* **1996**, *35*, 13147−13156.
(10) McCann, J. A. B.; Berti, P. J. *Chem. Rev.* **2006**, *106*, 506−555.
(11) Francis, A. W.; Helquist, S. A.; Kool, E. T.; David, S. S. *J. Am. Chem. Soc.* **2003**, *407*, 16235−16242.
(12) McCann, J. A. B.; Berti, P. J. *J. Am. Chem. Soc.* **2007**, *129*, 7055−7064.
(13) Chen, X. Y.; Berti, P. J.; Schramm, V. L. *J. Am. Chem. Soc.* **2000**, *122*, 1609−1617.
(14) Bryan, R. F.; Tomita, K. *Nature* **1961**, *192*, 812−814.
(15) Bryan, R. F.; Tomita, K. *Acta Crystallogr.* **1962**, *15*, 1179−1182.
(16) Saenger, W. In *Principles of Nucleic Acid Structure*, 6th ed.; Cantor, C. R., Ed.; Springer-Verlag: New York, 1984.
(17) Lavery, R.; Pullman, A.; Pullman, B. *B. Theor. Chim. Acta* **1978**, *50*, 67−73.
(18) Kampf, G.; Kapinos, L. E.; Griesser, R.; Lippert, B.; Sigel, H. J. *Chem. Soc., Perkin Trans.* **2002**, *2*, 1320−1327.
(19) Guan, Y.; Manuel, R. C.; Arvai, A. S.; Parikh, S. S.; Mol, C. D.; Miller, J. H.; Lloyd, R. S.; Tainer, J. A. *Nat. Struct. Biol.* **1998**, *5*, 1058−1064.
(20) Manuel, R. C.; Hitomi, K.; Arvai, A. S.; House, P. G.; Kurtz, A. J.; Dodson, M. L.; McCullough, A. K.; Tainer, J. A.; Lloyd, R. S. *J. Biol. Chem.* **1998**, *279*, 46930−46939.
(21) Miller, J. H.; Chiang, C. P.; Straatsma, T. P.; Kennedy, M. *J. Am. Chem. Soc.* **2003**, *125*, 6331−6336.
(22) Li, H.; Robertson, A. D.; Jensen, J. H. *Proteins: Struct., Funct., Bioinf.* **2005**, *61*, 704.
(23) Bas, D. C.; Rogers, D. M.; Jensen, J. H. *Proteins: Struct., Funct., Bioinf.* **2008**, *73*, 765.
(24) Olsson, M. H. M.; S£ndergaard, C. R.; Rostkowski, M.; Jensen, J. H. *J. Chem. Theory Comput.* **2011**, *7*, 525.
(25) Nosé, N. *J. Chem. Phys.* **1984**, *81*, 511−519.
(26) Martyna, G. J.; Tobias, D. J.; Klein, M. L. *J. Chem. Phys.* **1994**, *101*, 4177−4189.
(27) Feller, S. E.; Zhang, Y.; Pastor, R. W.; Brooks, B. R. *J. Chem. Phys.* **1995**, *103*, 4613−4621.
(28) Phillips, J. C.; Braun, R.; Wang, W.; Gumbart, J.; Tajkhorshid, E.; Villa, E.; Chipot, C.; Skeel, R. D.; Kale, L.; Schulten, K. *J. Comput. Chem.* **2005**, *26*, 1781−1802.
(29) Case, D. A.; Darden, T. A.; Cheatham, T. E.; Simmerling, C. L.; Wang, J.; Duke, R. E.; Luo, R.; Crowley, M.; Walker, R. C.; Zhang, W.; Merz, K. M.; Wang, B.; Hayik, S.; Roitberg, A.; Seabra, G. et al. *AMBER 10*; University of California: San Francisco, CA, 2008.
(30) Wang, J.; Cieplak, P.; Kollman, P. A. *J. Comput. Chem.* **2000**, *21*, 1049−1074.
(31) Hornak, V.; Abel, R.; Okur, A.; Strockbine, B.; Roitberg, A.; Simmerling, C. *Proteins* **2006**, *61*, 712−725.
(32) Car, R.; Parrinello, M. *Phys. Rev. Lett.* **1985**, *55*, 2471−2474.
(33) Laio, A.; VandeVondele, J.; Rothlisberger, U. *J. Chem. Phys.* **2002**, *116*, 6941−6948.
(34) Lee, C.; Yang, W.; Parr, R. G. *Phys. Rev. B* **1988**, *37*, 785−789.
(35) Becke, A. D. *Phys. Rev. A* **1988**, *38*, 3098−3100.
(36) Parrinello, M. *Solid State Commun.* **1997**, *102*, 107−120.
(37) Tuckerman, M.; Laasonen, K.; Sprik, M.; Parrinello, M. *J. Am. Chem. Soc.* **1995**, *99*, 5749−5752.
(38) Piana, S.; Carloni, P. *Proteins: Struct., Funct., Bioinf.* **2000**, *39*, 26−36.
(39) Molteni, C.; Parrinello, M. *J. Am. Chem. Soc.* **1998**, *120*, 2168−2171.
(40) De Vivo, M.; Dal Peraro, M.; Klein, M. L. *J. Am. Chem. Soc.* **2008**, *130*, 10955−10969.
(41) N., T.; Martins, J. L. *Phys. Rev. B* **1991**, *43*, 8861−8869.
(42) Lin, I.-C.; Coutinho-Neto, M. D.; Felsenheimer, C.; von Lilienfeld, O. A.; Tavernelli, I.; Rothlisberger, U. *Phys. Rev. B* **2007**, *75*, 205131.
(43) von Lilienfeld, O. A.; Sebastiani, D.; Tavernelli, I.; Rothlisberger, U. *Phys. Rev. Lett.* **2004**, *93*, 153004.

(44) Arey, J. S.; Aeberhard, P. C.; Lin, I.-C.; Rothlisberger, U. *J. Phys. Chem. B* **2009**, *113*, 4726−4732.
(45) Lin, I.-C.; Seitsonen, A. P.; Coutinho-Neto, M. D.; Tavernelli, I.; Rothlisberger, U. *J. Phys. Chem. B* **2009**, *113*, 1127−1131.
(46) von Lilienfeld, O. A.; Tavernelli, I.; Hutter, J.; Rothlisberger, U. *J. Chem. Phys.* **1988**, 122.
(47) Martyna, G. J.; Tuckerman, M. E. *J. Chem. Phys.* **1999**, 110.
(48) Sprik, M.; Ciccotti, G. *J. Chem. Phys.* **1998**, *109*, 7737−7744.
(49) JG, K. *J. Chem. Phys.* **1935**, *3*, 300−313.
(50) Giudice, E.; Várnai, P.; Lavery, R. *R. Nucleic Acid Res.* **2003**, *31*, 1434−14430.
(51) Carloni, P.; Rothlisberger, U.; Parrinello, M. *Acc. Chem. Res.* **2002**, *35*, 455−464.
(52) Laio, A.; Vandevondele, J.; Rothlisberger, U. *J. Phys. Chem. B* **2002**, *106*, 7300−7307.